



6th Underwater Acoustics Conference & Exhibition

20-25 June 2021

**Underwater Acoustics: Advances in acoustic
measurement systems: Technologies and
applications, hydrophone research.**

Acoustic vector sensor underwater communications in the Makai Experiment

Fabricio de Abreu Bozzi and Sérgio Manuel Machado Jesus

*Laboratory for Robotics and Engineering Systems (LARSys), University of Algarve, Faro, Algarve,
8005-139, PORTUGAL; fabriciobozzi@gmail.com; sjesus@ualg.pt*

The performance of a vector sensor array (VSA) receiving communication signals in the Makai experiment is quantified. The VSA composed of 4 vector sensors (VS) was tied to a drifting research vessel in shallow water. A bottom-moored source was used to transmit signals from 8k to 14kHz. In the present study, pressure and particle velocity channels are weighted-combined leading to a directional gain (VS beam steering). The communication chain for coherent modulation is composed of noise normalization, VS beam steering, synchronization, Doppler tracking, and a single Decision Feedback Equalizer.

The noise normalization step (denoising) is used since the noise power is not uniformly distributed among the pressure and velocity channels. This normalization emphasizes the vertical particle velocity, which benefit communication performance. Bit error rate (BER) performance is estimated for the pressure-only array, a single VS, and the VSA. It is shown that a single VS may provide similar communication performance to four pressure sensors. The BER for the shorter range (230m) varies from 0 to 5%, depending on the number of sensors used. It is noticed that in a multipath environment, steering to the Direction of Arrival (DoA) elevation may not lead to the lowest error for communications.

1. INTRODUCTION

Acoustic vector sensors (VS) for underwater applications have been widely investigated in the last three decades. In the 90s, VS studies were mostly directed to sonar applications, where source finding (or Direction of Arrival) methods were developed.^{1,2} However, recently, VS has been used in areas such as bioacoustic,^{3,4} seabed parameter estimation,⁵ and underwater acoustic communications (UWAC).^{6,7}

The motivation of VS usage is related to its compactness and the direction information provided by particle velocity. A vector sensor is a device that measures pressure and particle velocity. This last measure can be obtained by pressure-gradient or inertial sensors. The former uses pairs of omnidirectional hydrophones, and the latter uses accelerometers. Thus, a VS is composed of one hydrophone (pressure measurement) and an inertial/pressure-gradient sensor forming a co-located sensor.⁸

In this study, experimental results are based on accelerometer sensors (inertial). Accelerometer-based sensors to measure particle velocity have been used on waterway security and for communications.^{7,9} In those studies, this type of VS is tested for frequencies up to 15 kHz. However, there are gaps in the analysis of particle velocity channels, such as noise power, synchronization, Doppler tracking, and channel combining.

High-frequency signals used in UWAC systems may vary from a few kilohertz to hundreds of kilohertz. The UWAC issues, particularly in shallow water, can be summarized by attenuation, intersymbol interference (ISI) caused by multipath, and severe delay-Doppler spread.¹⁰ In this regard, a single vector sensor or an array of VS has shown superior communication performance to pressure-only arrays.^{6,11} Thus, the use of VS for UWAC is a promising topic, which experimental results are still limited.

This study quantifies the communication performance of a VSA in a field experiment. In this sea experiment, called MakaiEx, a VSA was tied to a research vessel, which drifted in a free trajectory. Communication signals were transmitted from a bottom-moored source. The VS communication performance is quantified for two source-receiver ranges (230 m and 910 m). Moreover, the impact of the quantity of VS used in the VSA is analyzed by the bit error rate (BER). The receiver signal processing chain is composed of noise normalization, VS beam steering, Doppler tracking, and a single Decision Feedback Equalizer (DFE).

Results show that noise power is not uniformly distributed among VS channels. A denoising approach aims to balance noise power of VS channels. This approach emphasizes the vertical component, which improves communication performance. The VS beam steering method, using estimated angles from DoA, is straightforward. This method presents reasonable performance for the shorter range, but it does not converge for the longer range. For a single VS, the performance is superior to three pressure-only sensors. The lowest BER is achieved using three VS elements, but a coherent combination issue was noticed. Finally, it is shown that due to multipath, using the elevation angle that points to the source does not necessarily result in the lowest error (in agreement with previous simulations¹²).

2. THEORETICAL FRAMEWORK

In this section, the basis of vector sensors for underwater communications is presented. First, the data model is presented. Then, VS as a receiver for communications is shown. Considerations regarding VS beam steering method, synchronization, Doppler tracking, and noise normalization are made.

A. DATA MODEL

The system equation for a single vector sensor can be defined as:

$$\begin{aligned}
r_p &= h_p \otimes s + w_p \\
r_{vx} &= h_{vx} \otimes s + w_{vx} \\
r_{vy} &= h_{vy} \otimes s + w_{vy} \\
r_{vz} &= h_{vz} \otimes s + w_{vz}
\end{aligned} \tag{1}$$

where s is the transmitted signal, $h_{(p/v)}$ are the channel impulse responses of pressure and particle velocity, and $r_{(p/v)}$ are the received pressure/pressure-equivalent particle velocity signals. For plane waves, pressure-equivalent particle velocity is the product of particle velocity by acoustic impedance ($\rho_0 c$, where ρ_0 is the static density and c the sound velocity). This is generally employed to combine pressure and particle velocity measures in the VS signal processing. The noise $w_{(p/v)}$ is assumed to be spherically isotropic.

B. VECTOR SENSORS AS A RECEIVER FOR COMMUNICATIONS

Vector sensor is a device that started to be explored in the underwater communication field recently. A single VS is a multi-channel system and authors try to take advantage of its inherent directional information.⁶ Figure 1 shows the proposed receiver for a single VS. This receiver adopts a beamforming approach. In the first step, noise normalization is performed. Then, the VS channels are weight-combined, where the weights are calculated according to estimated angles. In this sense, the DoA or the ‘‘optimum angle’’ is used. Then, resampling is performed in order to compensate Doppler shift. Finally, a DFE is used to reduce residual ISI.¹³ The DFE is composed of a feed-forward filter, a detector, a feedback filter, and an embedded second order phase-locked loop (PLL). The following sections explore the characteristic of each step.

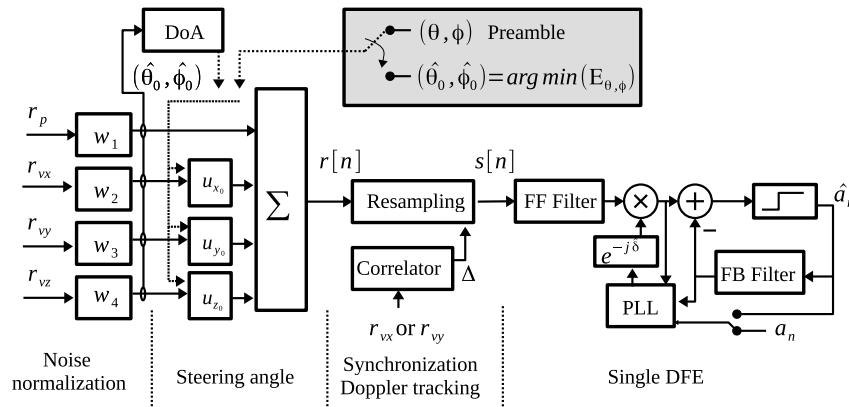


Figure 1: Single VS as a receiver for communications. θ and ϕ stand for azimuth and elevation angles.

i. Noise Normalization

In Fig. 1, the first step is the noise normalization. Commonly, noise power correlation, which is calculated through the auto and cross-covariances, is assumed to be isotropic (spherically decorrelated). In a single VS, this leads to the assumption that pressure noise power is equal to the sum of noise power velocity components.¹⁴ However, it is known that this assumption is not valid for multipath and reverberation scenarios.^{6,15} In a multipath environment, noise power may not be uniformly distributed among VS channels.¹⁶

Thus, the noise power analysis for a field experiment is necessary. Here, it is proposed to balance the noise power among pressure and particle velocity components by using the denoising approach.¹⁷

The denoising approach aims to compensate noisy channels. Maximum Likelihood Estimation was used as an alternative to a recursive noise power normalization (where iterative channel estimation is necessary).¹⁶ In this sense, low noise power channels are amplified, while noisy power channels are attenuated. The weight of channel m can be calculated according to:

$$w_m = \frac{\frac{1}{\sigma_m^2}}{\sum_{i=1}^K \frac{1}{\sigma_i^2}}, \quad (2)$$

where σ^2 is the noise power and K is the number of channels. The denoising effect is felt in terms of directivity pattern. Felisberto et al.¹⁸ have shown that combining pressure and z particle velocity component produce the output: $y_z = r_p(w_p + \sin(\phi))$. Thus, controlling w_p means a wide or a narrow beam pattern. A higher value of w_p amplifies the pressure channel, which makes the VS to reduce its directional pattern.

ii. Vector Sensor Beam Steering

The second step showed in Fig. 1 is composed of VS beam steering. This method weight-combines VS channels. The weights are calculated according to azimuth and elevation angles. The channels' combination produces a sensitivity pattern that points to the desired angle. In other words, a directional gain is produced in the desired direction. The signal output is given as:¹⁸

$$y = r_p + r_{vx} \cos(\theta_0) \cos(\phi_0) + r_{vy} \sin(\theta_0) \cos(\phi_0) + r_{vz} \sin(\phi_0), \quad (3)$$

where $r_{(p/v)}$ are the received pressure/pressure-equivalent particle velocity signals. The azimuth θ_0 and the elevation ϕ_0 are steering angles. The objective is to estimate angles that benefit the communication (i.e. result in the lowest error).

The first option is to steer to the source direction, and a DoA algorithm can be used. Several options for DoA estimation are found in the literature.^{2,18,19} However, a qualitative analysis among Intensity-based, Minimum Variance Distortionless Response (MVDR), and Bartlett beamforming shows that the latter presents a robust response to multipath, comparatively to the former methods. Thus, the Bartlett beamforming is used. The beam pattern response and the DoA estimation are given by:

$$\begin{aligned} B(\omega, \theta, \phi) &= \mathbf{v}^H \hat{\mathbf{R}} \mathbf{v} \\ (\hat{\theta}_0, \hat{\phi}_0) &= \arg \max \{B(\omega, \theta, \phi)\} \end{aligned} \quad (4)$$

where $\mathbf{v} \equiv \mathbf{v}(\omega, \theta, \phi)$ is the VS array manifold, $\hat{\mathbf{R}}$ is the estimated correlation matrix, and $[]^H$ is the Hermitian operator. For a single VS, $\mathbf{v} = [\mathbf{1} \ \mathbf{u}]^T$, where $\mathbf{u} = [\cos(\theta) \cos(\phi) \ \sin(\theta) \cos(\phi) \ \sin(\phi)]^T$. In Eq. 4, the estimated angles $(\hat{\theta}_0, \hat{\phi}_0)$ are obtained by the maximum of the beam response.

The DoA estimation approach is straightforward. However, simulations have shown that due to multipath the estimated elevation angle may not result in the lowest error (even if it points to the source direction).¹² The question that arises is: Is there an angle that brings the best performance (called here, optimum angle)? The gray box in Fig. 1 shows an option based on the minimum error. In this approach, instead of using the DoA, a range of angles is tested. The message preamble is used for training and to obtain the error $(E_{\theta, \phi})$. The angle that corresponds to the minimum value in the BER output map is chosen.

The VSA signal processing combines the vector sensors after resampling. Both DoA and optimum angle approaches are used. One can suggest performing delay-and-sum beamforming to enforce coherence, instead of summing. However, it is known that the used wavelength produces grating lobes, which degrades

the performance as well. For the optimum angle approach, the same estimated angle $(\hat{\theta}_0, \hat{\phi}_0)$ is used for all VS.

iii. Synchronization and Doppler Tracking

In Fig. 1, the third step is composed of synchronization and Doppler tracking. Symbol synchronization and Doppler tracking are challenging tasks in coherent underwater communication systems. There is no unique approach to overcome those issues. In short, the performance is related to the transmitted signal, its time bandwidth, and the received signal-to-noise ratio. In this work, the ambiguity method is used.²⁰ The Doppler distorted received signal in discrete-time can be modeled as:

$$r[nT_s] = s[(1 + \Delta)nT_s], \quad (5)$$

where s is the transmitted signal, Δ is the compression/expansion factor, and T_s is the sampling period. One can notice that Eq. 5 represents a noise free single path. In a multipath environment, the distorted received signal is a contribution of each delay-Doppler spread component of Eq. 5 type. However, if source-receiver relative motion is predominantly horizontal, Δ will be similar to all contributions, and compensating for a single Δ value may be sufficient.²¹

A pseudonoise (PN) m-sequence preamble is used as a replica in a Doppler search range. Then, the first arrival of the strongest correlator output is tracked along with subsequent interleaved packets. The Δ factor is estimated using the time difference between packets. Tracking the first arrival when it is not the strongest one along the packets may be a challenge. In shallow water, this effect can be noticed if the source or receiver is close to the seafloor.

The Doppler compensated received signal is given by:

$$s[nT_s] = r \left[\frac{nT_s}{(1 + \Delta)} \right]. \quad (6)$$

Equation 6 shows that a fractional sampling period is necessary to compensate for the time compression/expansion factor. This sample rate conversion can be performed using polyphase filters, which an efficient implementation is the *resample* Matlab function.

3. MAKAI'05 EXPERIMENT

MakaiEx'05 was a four-week field experiment, which took place off the coast of Kauai Island, Hawaii, in 2005. A vector sensor array was deployed receiving acoustic signals for different purposes (DoA, source localization, geoacoustics, and communications).²² The VSA used in the experiment is composed of five vector sensors TV-001 (Wilcoxon Research Inc.). Each vector sensor is made of three uni-axial accelerometers and one omnidirectional hydrophone. The accelerometers and the hydrophone are encapsulated, making a $3,81 \times 6,35$ cm neutrally buoyant cylinder-type. The spacing between VS is 10 cm.

Figure 2a shows a 3D illustration of the scenario. The VSA was tied at the stern of the research vessel Kilo Moana. It was held by a cable at 40 m depth. A 100-150 kg weight was used at the bottom extremity of the cable to keep the VSA as close to vertical as possible. The sound speed varied between 1528 m/s and 1538 m/s over its vertical profile (see the sound speed profile - SSP, in Figure 2a). The data analyzed here refers to the communication test performed on September 23rd. For this day, a source was transmitting at 90 m depth (104 m water depth). Since one of the VS (the bottom extremity one) did not work properly during the experiment, only four VS data are available.

Transmissions were performed during a vessel drift. Figure 2b shows the vessel GPS track in x-y range, taking as reference the drift end position. In this figure, the source is highlighted as a yellow dot. The arrows

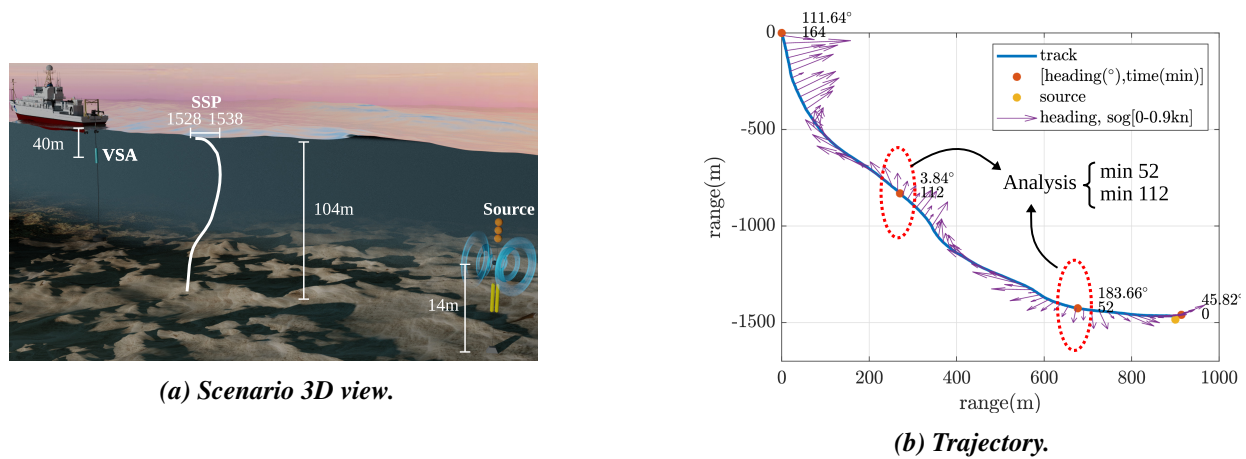


Figure 2: MakaiEx scenario.

are vessel headings along time, which arrow amplitudes are set according to the speed over ground (sog). Red dots are the vessel’s position when the data recording starts and finishes. For these instants, source-vessel ranges are approximately 20 m and 1736 m, respectively. Red circles highlight the ship’s position for two recording instants analyzed in the present study.

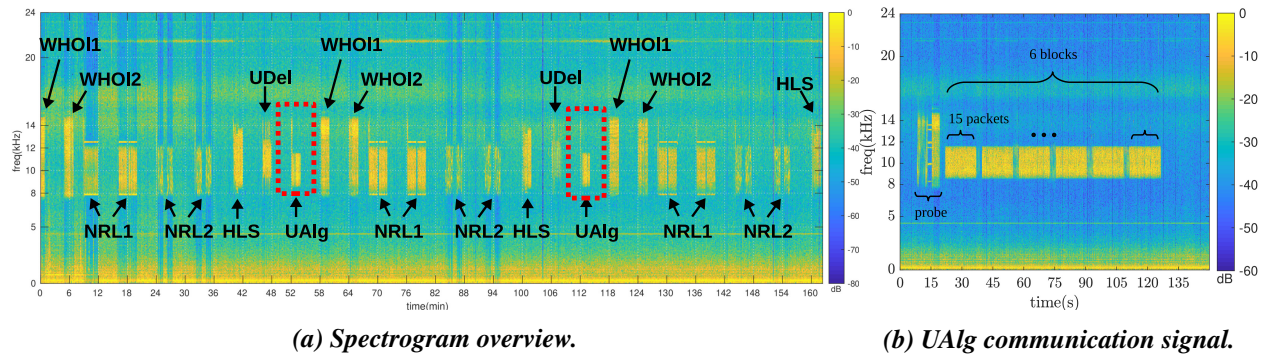


Figure 3: Pressure channel received signal.

Several institutions participating in the MakaiEx transmit different types of modulations, at specific timestamp (see Fig. 3a). The signal analyzed here (from the University of Algarve - UAlg) refers to minutes 52 and 112. Figure 3b shows the spectrogram of UAlg received signal. The source-VSA ranges for these timestamps are approximately 230 m and 907 m, respectively. The UAlg communication signal is composed of the main probe and 6 blocks. Each block contains 15 packets of 1 s. Each packet contains 2000 symbols (BPSK), the first 127 of them are a m-sequence. This m-sequence is used for Doppler tracking and time synchronization.

4. RESULTS AND ANALYSIS

A. SYNCHRONIZATION AND DOPPLER TRACKING

The first step to symbol synchronization is to find the strongest arrival of the correlator output. The Doppler frequency range is set ± 10 Hz, and the search step is 0.2 Hz. Figure 4a shows the correlator output

for two consecutive packets (pkt 4 and 5). If the strongest arrival was chosen, the third arrival would be chosen for packets 4 and 5. The time instant of these peaks is shown in dashed line of Fig. 4b. Note that the time expansion estimation would not be correct using the strongest arrivals. Thus, the first arrival is chosen. Selecting the time of the first arrival results in a “soft” expansion/compression curve, as shown in solid line of Fig. 4b.

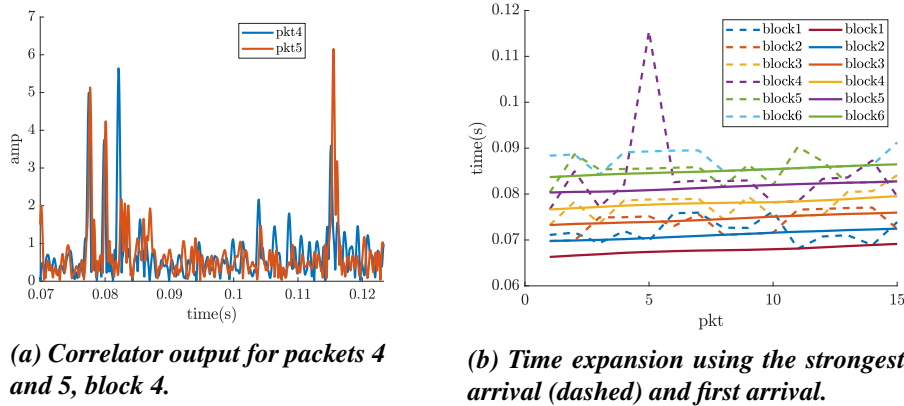


Figure 4: Symbol synchronization and Doppler factor estimation.

Figure 4b shows that there is time expansion, since the curve grows (solid line). If there was not Doppler all lines would be horizontal. The Doppler factor Δ is the time difference between two sequential packets. For the last packet of each block the last calculated Δ is used.

The search for the first arrival may be difficult when several arrivals are close to each other with similar amplitudes. Moreover, another issue arises if the direct path is not the first arrival (the strongest amplitude is not the first peak). In this sense, using the horizontal particle velocity component is advantageous to filter arrivals from steeper angles.

B. DENOISING

In field experiments, the noise power can be calculated using the interval among transmissions. The denoising analysis is shown in Fig. 5. It was not expected a high noise power variation due to the ship’s self noise (dynamic positioning system and auxiliary machinery). However, Fig. 5a shows a large power difference for the data until minute 31 to the rest of the data. It is known that the ship tried to keep a specific positioning to the source until around minute 30. This is indicative that the dynamic positioning system could be active. This fact is also noticed by the spectrogram of the VS vertical component in Fig. 5b. This spectrogram shows the sharp noise reduction at min 30,9. The result of this sharp variation is felt by the denoising weights shown in Fig. 5c. Thus, the estimated weight used in the receiver is the mean value ignoring the initial interference.

Another verified characteristics regards to the pressure and the vertical particle velocity noise power. One can notice that the power of these channels are low comparing to the horizontal components. Thus, the gain provided for these channels tends to balance the noise power.

C. COMMUNICATION PERFORMANCE

The communication performance is analyzed for the pressure-only array, a single VS, and the VSA. The bit error is used to quantify the performance. Figure 6 shows the estimated Channel Impulse Response (CIR) before and after alignment for the y component of VS #4. The CIR presented in these figures join’s the 6

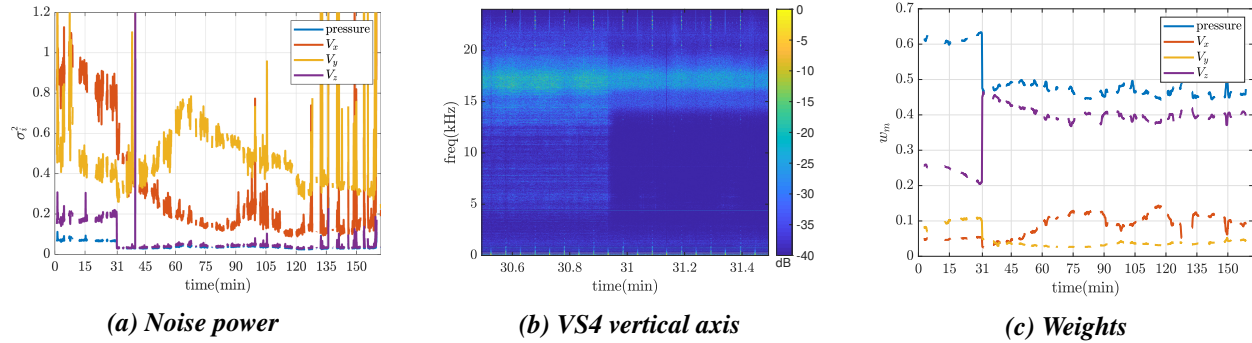


Figure 5: Denoising analysis

blocks. The total time (sometimes referred to as geotime) is 90 s (15 s of each block). Time expansion is noticed as well as the time discontinuity between blocks (due to blank intervals among blocks). A time expansion of about 15 ms may be considered small compared to 1 min 30 s. Anyhow, Doppler compensations is proved necessary.

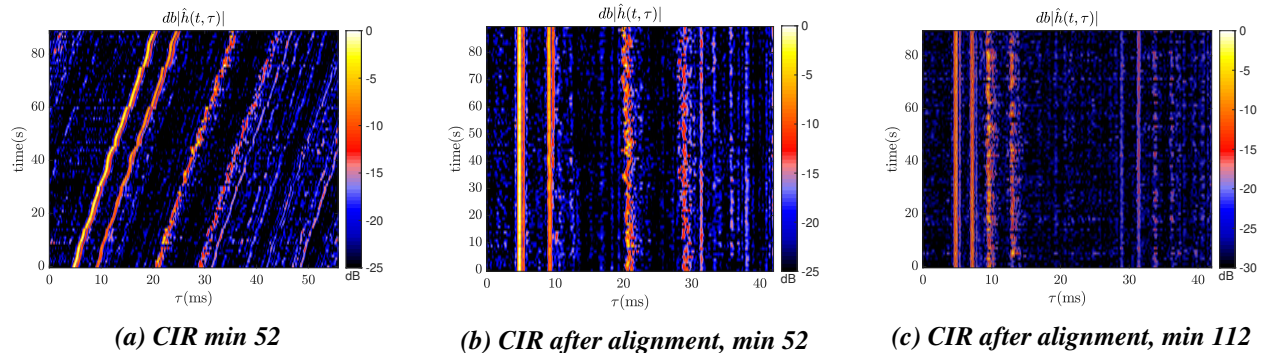


Figure 6: CIR VS4 y-component for minutes 52 and 112

Fig. 7a shows the communication performance as BER versus the number of sensors. The pressure-only combination is performed after individual synchronization. Performance varies from 9% to 5% combining sensor #4 to #2. The BER indicates that non-coherent combination degrades the performance. This is noticed when summing more than three sensors. In this study, coherence combination issues is not addressed.

Vector sensor #4 is used to quantify the performance of a single VS. In order to verify the impact of the denoising, the BER performance is presented with and without denoising. When the denoising is not used, the BER performance varies from 6% to 0.1% (no denoising/no ref). One can notice the estimated elevation not using the denoising in Fig. 7b. The estimated angle is about 5° and there is no high angle fluctuation. This result is due to z-component attenuation, as seen in the noise power calculation. Thus, the BER performance gain is mainly due to horizontal particle velocity channels.

Since the denoising increases the z-component gain, more sensitivity to surface and bottom reflections is felt in the estimated elevation. This can be seen by the high angle fluctuation in Fig. 7b when the denoising is used. Moreover, each vector sensor estimates distinct angles. This effect degrades the BER performance combining more than two VS, as shown in Fig. 7a (denoising/no ref).

One adopted strategy is to use one VS as reference. Figure 7a shows the performance using denoising and the VS #4 as reference (denoising/ref). The coherence combination issue is partially solved and the performance varies from 3% to 0.1%.

At last, Fig. 7c shows the BER map for a range of angles. It is possible to verify the direction (“optimum

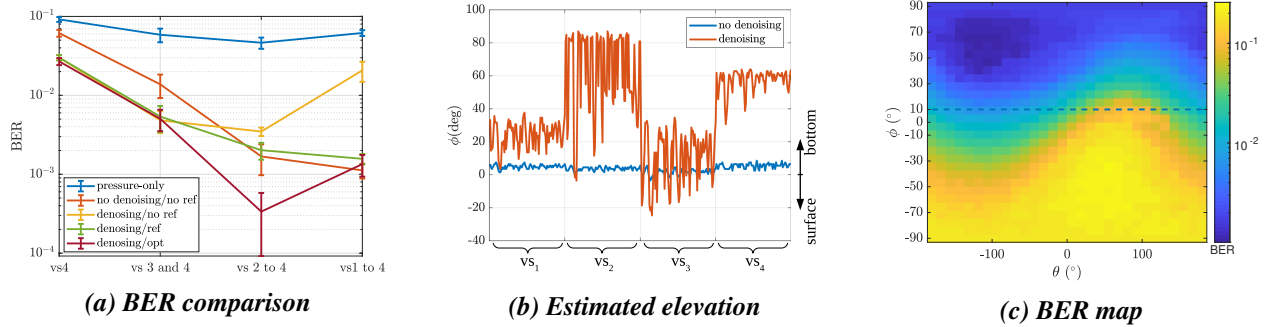


Figure 7: VSA performance comparison, minute 52

angle”) that results in the minimum BER. One can notice that the elevation angle is not the direct path angle ($\approx 10^\circ$). Selecting the optimum angle for each VS combination results in the BER from 3% to 0.01% (combining VS #4 to #2). Since the coherence combination is not treated, the performance decreases using VS #1.

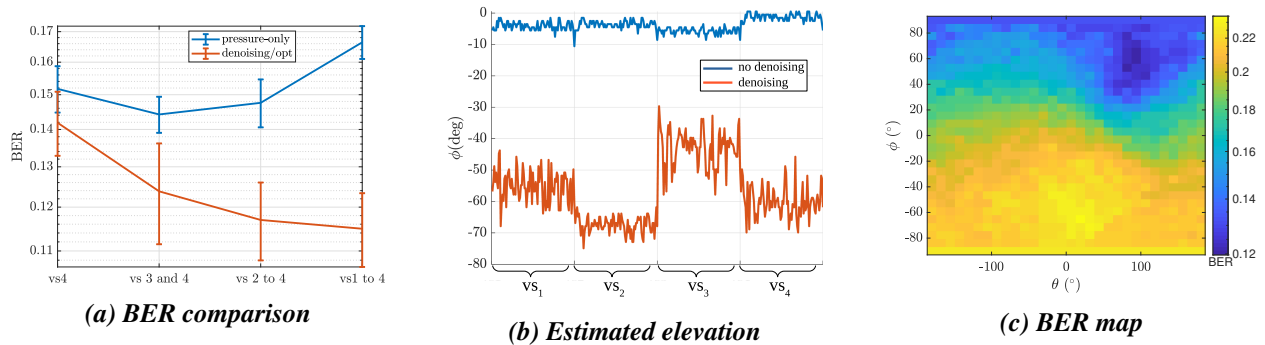


Figure 8: VSA performance comparison, minute 112

Figure 8 shows the VSA performance for minute 112. Figure 8a shows the pressure-only and the optimum angle BER performance. The result using DoA estimation does not converge (not shown in the figure). The explanation for non convergence is related to the estimated elevation angles, which are negatives (see Figure 8b, using denoising). Thus, one can notice that using negative angles (surface direction) results in higher error, as shown in Fig. 8c.

BER performance for the pressure-only array suggests that the combination is not coherent, which degrades the performance. Using the optimum angle, according to the BER map of Fig. 8c, results in lower error. Minute 112 performance can be justified by the signal-to-noise ratio and the challenging channel (see Fig. 6c). The SNR is from 3 dB to 10 dB lower than the SNR for min 52 (depending of the channel). This lower SNR may justify equalizer convergence failures, which reduce the DFE benefit.

5. CONCLUSION

In this study, vector sensor array communication performance is quantified in a challenging field experiment. Coherent modulation was used taking advantage of efficient bandwidth usage. The vector sensor was considered as an intensity sensor. Thus, its channels were combined using the VS beam steering method, which acts as a spatial filter.

Results have confirmed the outperformance of VS over a pressure-only array, as demonstrated in previous theoretical studies. One VS presents equivalent performance to four pressure sensors. For the used array

geometry, it represents a 67% of length reduction ($\approx 1/3$), which is an attractive VS characteristic. Noise normalization was adopted, since noise power was not uniformly distributed among particle velocity and pressure channels. It was shown that the pressure and vertical particle velocity component were amplified. The gain provided for these channels results in an additional benefit. However, it was also highlighted that coherence combination when using multiple VS may degrades the BER performance. At last, an “optimum” angle can be found according to minimum of the BER map. This analysis shows that in a multipath environment pointing to the source not necessarily results in the lowest error.

ACKNOWLEDGMENTS

The authors would like to thank Makai’s research group: M. Porter (chief scientist), J. Tarasek (vector sensor array), P. Hursky, M. Siderius and B. Abraham (data acquisition assistance). The Makai Experiment was supported by ONR. The Ph.D student is supported by the Postgraduate Study Abroad Program of the Brazilian Navy, Grant No. Port. 227/MB/2019.

This work was funded by National Funds through Foundation for Science and Technology (FCT) - LARSyS (Project UIDB/50009/2020).

REFERENCES

- ¹ J. Nickles, G. Edmonds, R. Harriss, F. Fisher, W. Hodgkiss, J. Giles, and G. D’Spain, “A Vertical Array Of Directional Acoustic Sensors,” in *OCEANS 92 Mastering the Oceans Through Technology*, vol. 1, (Newport, RI), pp. 340–345, IEEE, 1992.
- ² A. Nehorai and E. Paldi, “Acoustic vector-sensor array processing,” *IEEE Transactions on Signal Processing*, vol. 42, pp. 2481–2491, Sept. 1994.
- ³ S. L. Nedelec, J. Campbell, A. N. Radford, S. D. Simpson, and N. D. Merchant, “Particle motion: the missing link in underwater acoustic ecology,” *Methods in Ecology and Evolution*, vol. 7, pp. 836–842, July 2016.
- ⁴ S. M. Jesus, F. C. Xavier, R. P. Vio, J. Osowsky, M. V. S. Simões, and E. B. F. Netto, “Particle motion measurements near a rocky shore off Cabo Frio Island,” *The Journal of the Acoustical Society of America*, vol. 147, pp. 4009–4019, June 2020.
- ⁵ P. Santos, J. Joao, O. C. Rodriguez, P. Felisberto, and S. M. Jesus, “Geometric and seabed parameter estimation using a vector sensor array - Experimental results from Makai experiment 2005,” in *OCEANS 2011 IEEE - Spain*, (Santander, Spain), pp. 1–10, IEEE, June 2011.
- ⁶ A. Abdi, H. Guo, and P. Sutthiwan, “A New Vector Sensor Receiver for Underwater Acoustic Communication,” in *OCEANS 2007*, (Vancouver, BC), pp. 1–10, IEEE, Sept. 2007. ISSN: 0197-7385.
- ⁷ A. Song, A. Abdi, M. Badiy, and P. Hursky, “Experimental Demonstration of Underwater Acoustic Communication by Vector Sensors,” *IEEE Journal of Oceanic Engineering*, vol. 36, pp. 454–461, July 2011.
- ⁸ C. H. Sherman and J. L. Butler, *Transducers and arrays for underwater sound*. Monograph series in underwater acoustics, New York: Springer, 2007.
- ⁹ J. Shipps and B. Abraham, “The use of vector sensors for underwater port and waterway security,” in *ISA/IEEE Sensors for Industry Conference, 2004. Proceedings the*, (New Orleans, LA, USA), pp. 41–44, IEEE, 2004.

- ¹⁰ M. Chitre, S. Shahabudeen, and M. Stojanovic, "Underwater Acoustic Communications and Networking: Recent Advances and Future Challenges," *Marine Technology Society Journal*, vol. 42, pp. 103–116, Mar. 2008.
- ¹¹ L.-x. Guo, X. Han, J.-w. Yin, and X.-s. Yu, "Underwater Acoustic Communication by a Single-Vector Sensor: Performance Comparison Using Three Different Algorithms," *Shock and Vibration*, vol. 2018, pp. 1–8, Nov. 2018.
- ¹² F. A. Bozzi and S. M. Jesus, "Vector Sensor Beam Steering for Underwater Acoustic Communications," in *Proceedings of Meetings on Acoustics*, vol. 42, p. 070002, ASA, 2020.
- ¹³ M. Stojanovic, J. Catipovic, and J. Proakis, "Phase-coherent digital communications for underwater acoustic channels," *IEEE Journal of Oceanic Engineering*, vol. 19, pp. 100–111, Jan. 1994.
- ¹⁴ M. Hawkes and A. Nehorai, "Acoustic vector-sensor correlations in ambient noise," *IEEE Journal of Oceanic Engineering*, vol. 26, pp. 337–347, July 2001.
- ¹⁵ D. Levin, E. A. P. Habets, and S. Gannot, "On the angular error of intensity vector based direction of arrival estimation in reverberant sound fields," *The Journal of the Acoustical Society of America*, vol. 128, pp. 1800–1811, Oct. 2010.
- ¹⁶ A. Song, M. Badiy, P. Hursky, and A. Abdi, "Time reversal receivers for underwater acoustic communication using vector sensors," in *OCEANS 2008*, (Quebec City, QC, Canada), pp. 1–10, IEEE, Sept. 2008.
- ¹⁷ G. F. Knoll, *Radiation detection and measurement*. New York: Wiley, 2nd ed ed., 1989.
- ¹⁸ P. Felisberto, P. Santos, and S. M. Jesus, "Acoustic Pressure and Particle Velocity for Spatial Filtering of Bottom Arrivals," *IEEE Journal of Oceanic Engineering*, vol. 44, pp. 179–192, Jan. 2019.
- ¹⁹ J. Cao, J. Liu, J. Wang, and X. Lai, "Acoustic vector sensor: reviews and future perspectives," *IET Signal Processing*, vol. 11, pp. 1–9, Feb. 2017.
- ²⁰ B. Sharif, J. Neasham, O. Hinton, and A. Adams, "A computationally efficient Doppler compensation system for underwater acoustic communications," *IEEE Journal of Oceanic Engineering*, vol. 25, pp. 52–61, Jan. 2000.
- ²¹ J. Gomes, A. Silva, and S. Jesus, "Joint Passive Time Reversal and Multichannel Equalization for Underwater Communications," in *OCEANS 2006*, (Boston, MA), pp. 1–6, IEEE, Sept. 2006.
- ²² M. Porter, B. Abraham, M. Badiy, M. Buckingham, T. Folegot, P. Hursky, S. Jesus, B. Kraft, V. McDonald, and W. Yang, "The Makai Experiment: High-Frequency Acoustics," in *ECUA*, (Carvoeiro, Portugal), p. 10, June 2006.